OPEN ACCESS

Hybrid Anode Design of Polymer Electrolyte Membrane Water Electrolysis Cells for Ultra-High Current Density Operation with Low Platinum Group Metal Loading

To cite this article: Masahiro Yasutake *et al* 2023 *J. Electrochem. Soc.* **170** 124507

Journal of The Electrochemical Society, 2023 **170** 124507

Hybrid Anode Design of Polymer Electrolyte Membrane Water Electrolysis Cells for Ultra-High Current Density Operation with Low Platinum Group Metal Loading

Masahiro Yasutake,[1,2] Zhiyun Noda,[3] Junko Matsuda,[2,3,4] Stephen M. Lyth,[2,5] Masamichi Nishihara,[2] Kohei Ito,[1,2,3] Akari Hayashi,[1,2,3,4,*] and Kazunari Sasaki[1,2,3,4,*,z]

[1]*Department of Hydrogen Energy Systems, Faculty of Engineering, Kyushu University, Nishi-ku, Fukuoka 819-0395, Japan*
[2]*Next-Generation Fuel Cell Research Center (NEXT-FC) Kyushu University, Nishi-ku, Fukuoka 819-0395, Japan*
[3]*International Research Center for Hydrogen Energy, Kyushu University, Nishi-ku, Fukuoka 819-0395, Japan*
[4]*Platform of Inter/ Transdisciplinary Energy Research (Q-PIT), Kyushu University, Nishi-ku, Fukuoka 819-0395, Japan*
[5]*Department of Chemical and Process Engineering, University of Strathclyde, Glasgow G1 1XL, United Kingdom*

Reducing platinum group metal (PGM) loading and high current density operation are both essential for minimizing the capital expenditure (CAPEX) of polymer electrolyte membrane (PEM) electrolyzers. Catalyst-integrated porous transport electrodes (PTEs) in which iridium acts as both a catalyst and a conductive coating on porous transport layer (PTL) surfaces, enable the preparation of Pt-coating-free PTLs, but can also result in relatively high activation and ohmic overvoltages. Here, a novel hybrid anode design combining an intermediate catalyst layer and a catalyst-integrated PTE is developed. This hybrid anode demonstrates that Ir on PTL can contribute to the oxygen evolution reaction (OER) and exhibits comparable electrolysis performance to a conventional anode consisting of Pt-coated PTL with the same Ir loadings despite Pt-coating-free on the PTL of the hybrid anode. This novel anode eliminates the need for a Pt coating whilst also enabling ultra-high current density operations up to 20 A cm^{-2} with a total PGM loading of only around 0.6 mg cm^{-2} on the anode side. This paper proposes a next-generation anode structure with new functions of PTLs for ultra-high current density operation with low PGM loading to significantly reduce green hydrogen costs.

 [DOI: 10.1149/1945-7111/ad1165]

Manuscript submitted January 4, 2023; revised manuscript received September 26, 2023. Published December 8, 2023.

Worldwide momentum for achieving carbon neutrality by 2050 is increasing at pace. Significant introduction of renewable energy is required to realize carbon neutrality at a global scale. Energy storage technologies are essential for building a robust electricity grid in a carbon-neutral society since power generation from renewable energy, such as solar and wind, depends on weather conditions. Green-hydrogen-centered power systems, where hydrogen acts as a renewable chemical energy carrier, are an ideal solution against the fluctuation in power supply from renewable electricity. In addition, renewable hydrogen can contribute to the decarbonization of the chemical, steel, and aviation industries which are difficult to electrify.[1,2]

Water electrolysis is a critical technology for the production of green hydrogen. Polymer electrolyte membrane water electrolysis (PEMWE) is characterized by its ability to produce highly pure hydrogen at high current density, low temperature, and even high pressure. In addition, there is fast load response of robust water electrolysis systems which can closely follow fluctuations in renewable energy. The current issue with green hydrogen is its higher cost compared to conventional fossil fuels and fossil fuel-derived hydrogen. Reducing the cost of green hydrogen is critical for promoting carbon neutrality. The total cost for producing green hydrogen is a sum of operation expenses (OPEX) related to renewable electricity and capital expenditure (CAPEX) of the electrolysis system. Currently, the dominant cost factor in the production of green hydrogen is the OPEX, but renewable electricity costs have decreased significantly in the past decade.[3] For example, wind power generation cost has been reduced by 30%–40%, and photovoltaic power generation cost by about 80% from 2010 to 2019.[3] Therefore, reduction in CAPEX is becoming increasingly important for the next generation of electrolyzers. The higher CAPEX of PEM electrolyzers prevents market penetration compared to the cheaper technology of alkaline electrolyzers. As such, reductions in CAPEX are essential for enhancing the competitiveness of PEM electrolyzers.

One critical factor for reduction of the CAPEX of PEM electrolyzers is to decrease the PGM loading. Currently, around 1 to 5 mg cm^{-2} of iridium-based catalyst (electrocatalyst) is used for the rate-determining anodic oxygen evolution reaction (OER).[2] In addition, platinum coating is applied to the anode-side PTL to prevent decreases in conductivity via PTL oxidation in the highly anodic potential and strongly acidic environment. Many research activities focus on improving the catalytic activity in order to reduce the iridium-based catalyst loading.[4–7] However, reducing the Pt coating on the PTL is also critical regarding the overall PGM loading within the electrolyzer. According to reports by the International Renewable Energy Agency (IRENA), 1 to 5 mg cm^{-2} of Pt is typically used as a coating to prevent the oxidization of titanium-based PTL and thereby cell performance degradation.[2] The PGM loading on the anode PTL is in fact comparable to that of the PGM catalyst loading. Despite this, the Pt coating has not received much attention in the literature. Since reducing the CAPEX of PEM electrolyzers is essential, significantly reducing the Pt coating on the anode or developing an alternative Pt-free PTL is important for reducing the total PGM loading.[8,9]

Noble metal loading can be reduced by increasing its catalytic activity and utilization. However, there is often a tradeoff between this and performance degradation. At low iridium loading, the ohmic overvoltage and activation overvoltage often significantly increase. A non-uniform catalyst layer also exhibits high overvoltages for catalyst layers with low Ir loading. This non-uniform catalyst layer causes low in-plain conductivity, leading to a high contact resistance between the catalyst layer and the PTL, and an associated reduction in catalyst utilization.[10–12]

Previously, Schuler et al. investigated cell performance degradation associated with contact resistance at the interface between the catalyst layer and the PTL.[11,12] Their study quantified the contact area of the interface using 3-dimensional imaging with X-ray computed tomography and image processing. They then evaluated

*Electrochemical Society Member.
[z]E-mail: sasaki@mech.kyushu-u.ac.jp

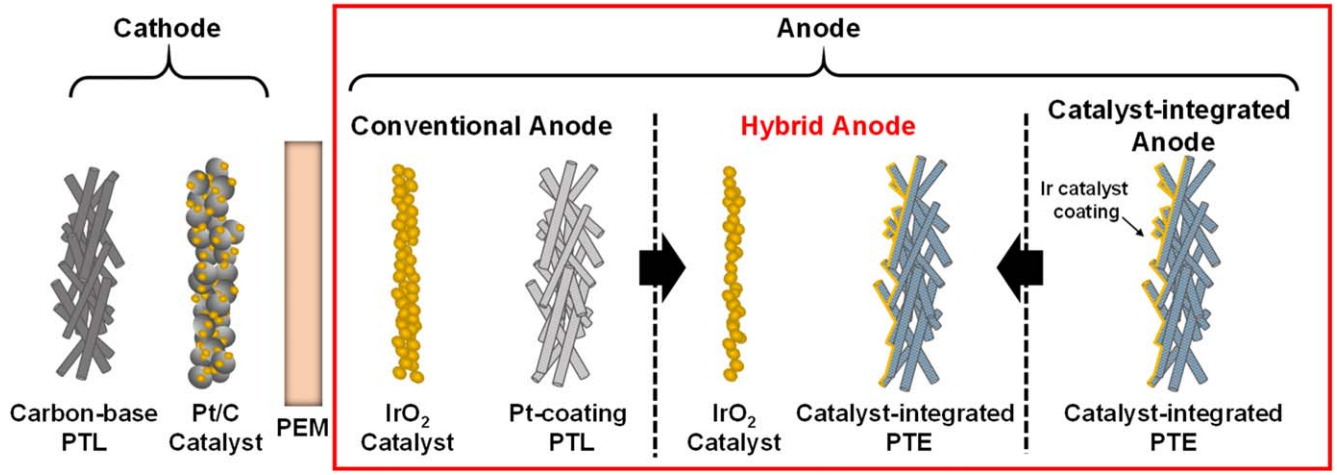

Figure 1. Schematic diagram of the hybrid anode concept with the conventional catalyst layer and catalyst-integrated PTE after Yasutake et al.[22] No Pt coating on PTL is made in this anode design because Ir on catalyst-integrate PTE acts as both an electrocatalyst and a conductive coating on PTL.

the correlation between the contact area and each overvoltage. According to their study, the ohmic overvoltage increased with decreasing the contact area between the catalyst area and the PTL due to the increase in contact resistance. Simultaneously, the decrease in the contact area decreases the catalyst utilization leading to increases in both the activation and mass transport overvoltages. Therefore, the interface between the catalyst layer and the PTL is one of the critical factors in determining PEMWE cell performance.[11,12]

Effects at the interface between the catalyst layer and the PTL become even more pronounced at a lower catalyst loading.[13,14] For example, Bernt et al. studied the effect of Ir loading on cell performance from 0.2 to 5.41 mg cm^{-2}.[13] A significant increase in the Tafel slop was observed with decreasing Ir loading, indicating an increase in activation overvoltage. In addition, an increase in high-frequency resistance, i.e., ohmic overvoltage increase, was also observed. This study concluded that the increase in these overvoltages is due to non-uniform catalyst layers of the cells at very low catalyst loadings, resulting in lower in-plane conductivity of the catalyst layer. These results suggest the importance of uniform catalyst layer preparation at low Ir loadings and electronic conduction at the interface between the catalyst layer and the PTL.

The Pt coating on the PTL also significantly affects the interfacial contact between the catalyst layer and the PTL. Again, Bernt et al. evaluated the effects of the presence or absence of the Pt coating and the conductivity of the catalyst on the initial PEMWE cell performance.[15] They evaluated and compared the impact of Pt coating on cell performance when using a low conductivity but high activity amorphous IrO(OH)x catalyst and a high conductivity but low activity IrO_2/TiO_2 catalyst. A significant cell performance degradation originating from the increase in activation overvoltage and ohmic overvoltage was observed when using the lower conductivity amorphous IrO(OH)x catalyst and the Pt-coating-free PTL compared to when using the higher conductivity IrO_2/TiO_2 catalyst. In other words, without the Pt coating on PTL, the contact resistance between the less conductive amorphous catalyst layer and the PTL increases and catalyst utilization decreases, resulting in a significant increase in activation overvoltage.[15]

These studies suggest that the effect of Pt coating on PTL performance may be more pronounced at low Ir-based catalyst loadings, where the in-plane conductivity of the catalyst layer is low. This suggests that it is difficult to simultaneously achieve both Pt-coating-free and low Ir catalyst loading using current cell structural designs. A novel anode design strategy is therefore necessary for significant PGM loading reduction on the PEMWE anode.

High current density operation is also an effective strategy for reducing the CAPEX of PEM electrolyzers. Although higher current density contributes to lower CAPEX, it simultaneously increases the OPEX because the efficiency of electrolysis is lower in this regime, due to various overvoltages. Therefore, optimization of the operating conditions is needed regarding current density and overvoltage. Villagra et al. determined that 2 to 3 A cm^{-2} at 2 V is the optimum current density for conventional water electrolysis cell performance, based on the conflicting CAPEX and OPEX relationships with the operating current density as a variable.[16] Higher current density of 10 A cm^{-2} is expected in the future. According to IRENA reports, PEMWE cells today are operated with a nominal current density of 1 to 2 A cm^{-2} and a load range between 5% to 120%. In 2050, a nominal current density of 4 to 6 A cm^{-2} and a load range of 5% to 300% are expected. In other words, a maximum current density of about 18 A cm^{-2} is required.[2]

Based on the considerations above, there are three possible strategies for reducing CAPEX in PEM water electrolyzers: (i) reducing the iridium catalyst loading; (ii) reducing the platinum coating on the PTL; and (iii) reducing the total electrode area by increasing the operating current density.

Our research group has developed a catalyst-integrated porous transport electrode, in which iridium catalysts are directly deposited on PTLs to resolve the above issues.[17–22] Figure 1 compares various cell structures with the conventional IrO_2 catalyst layers and the catalyst-integrated PTE,[22] and the hybrid anode concept to be examined in this study. Yasutake et al. treated Ti-based PTL with NaOH solution to form needle-like TiO_2 nanostructures with a high aspect ratio on the PTL surfaces,[22] increasing the surface area and enabling the PTL to act as a catalyst support. Arc plasma deposition was applied to prepare the catalyst-integrated PTE with Ir supported on a surface-modified PTL. This PTE structure, with iridium catalyst directly deposited on PTL,[22] enables to improve catalyst utilization. This electrode structure resulted in high electrolysis performance even at a total PGM usage below 0.2 mg cm^{-2} on the anode side because iridium acts as both a catalyst and a conductive coating in this PTL structure.

Here, we first evaluate the current-voltage (I-V) characteristics of this catalyst-integrated PTE at high current densities above 10 A cm^{-2}, comparing the performance with a conventional MEA structure. As described in Fig. 1, we also develop a novel hybrid anode design by applying the catalyst-integrated PTE as a PTL and inserting an intermediate catalyst layer for high current density operation under low electrolysis voltage. This structure has the following advantages. Currently, 1 to 5 mg cm^{-2} of Ir catalyst and 1 to 5 mg cm^{-2} of Pt coating on PTL are typically used in the PEMWE anode.[2] Consequently, the total PGM loading on the anode reaches 2 to 10 mg cm^{-2}. A catalyst-integrated PTE needs no platinum coating because deposited iridium plays the dual role of catalyst and

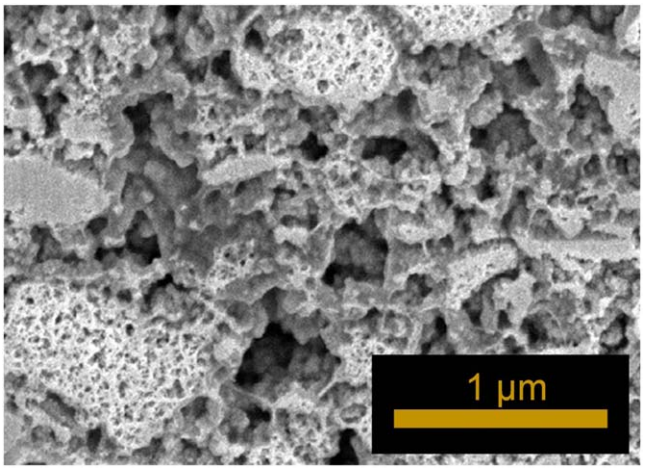

Figure 2. FIB-SEM image of a conventional IrO_2 catalyst layer, which is also applied for an intermediate catalyst layer of the hybrid anode.

conductive coating. The catalyst-integrated PTE could therefore have high mass activity with high ECSA at low Ir loadings. However, the ECSA and mass activity decreased with increasing Ir loading because Ir was deposited as a film at a high Ir loading.[22] Therefore, although the PTE exhibits high activity in low Ir loading regions, the activation overvoltage remains relatively high with increasing Ir loading. In the hybrid anode, where an intermediate catalyst layer is inserted between the electrolyte membrane and the catalyst-integrated PTE, both the intermediate catalyst layer and the catalyst-integrated PTE contribute to the oxygen evolution reaction (OER). The intermediate catalyst layer has the same function as a conventional catalyst layer, as shown in Fig. 2. Therefore, eliminating Pt from the PTL can lead to a reduction in the total PGM loading for cells in hybrid anodes compared with conventional anodes with the same Ir loading and electrolysis performance. This paper examines various functions of PTLs in PEMWE cells and provides a novel hybrid concept of anode design by adding OER activity to PTLs. The possibilities and issues in reducing the CAPEX of PEM water electrolyzers by using low PGM loadings and operating at high current densities under low voltages are discussed.

Experimental

Preparation of catalyst-integrated PTEs.—The procedure for preparing the catalyst-integrated PTEs is summarized in Fig. 3. Titanium microfiber sheets with nominal porosity of ca. 70% (Nikko Techno Ltd, Osaka, Japan) were used as PTLs. The average porosity of specimens determined by measuring their thickness and weight was 75.1 ± 2%. Some inaccuracy may arise from, e.g., the surface roughness of such porous materials, affecting their thickness measured by a micrometer. The titanium microfiber sheets have ca. 200 μm thickness and are made up of interconnecting titanium microfibers with individual cross sections of approximately 10 μm by 10 μm.[22]

In order to increase the surface area of the titanium PTLs, chemical etching with NaOH solution was performed.[22] First, titanium sheets were etched in an aqueous 1 M NaOH solution (Kishida Chemical Co., Ltd, Osaka, Japan) at 60 °C for 1 h. After that, the etched titanium sheets were washed under ultra-sonication in 0.01 M HNO_3 solution (Kishida Chemical Co., Ltd, Osaka, Japan) for 30 min, and then washed in deionized water at room temperature for 10 min for complete neutralization. Heat treatment was then

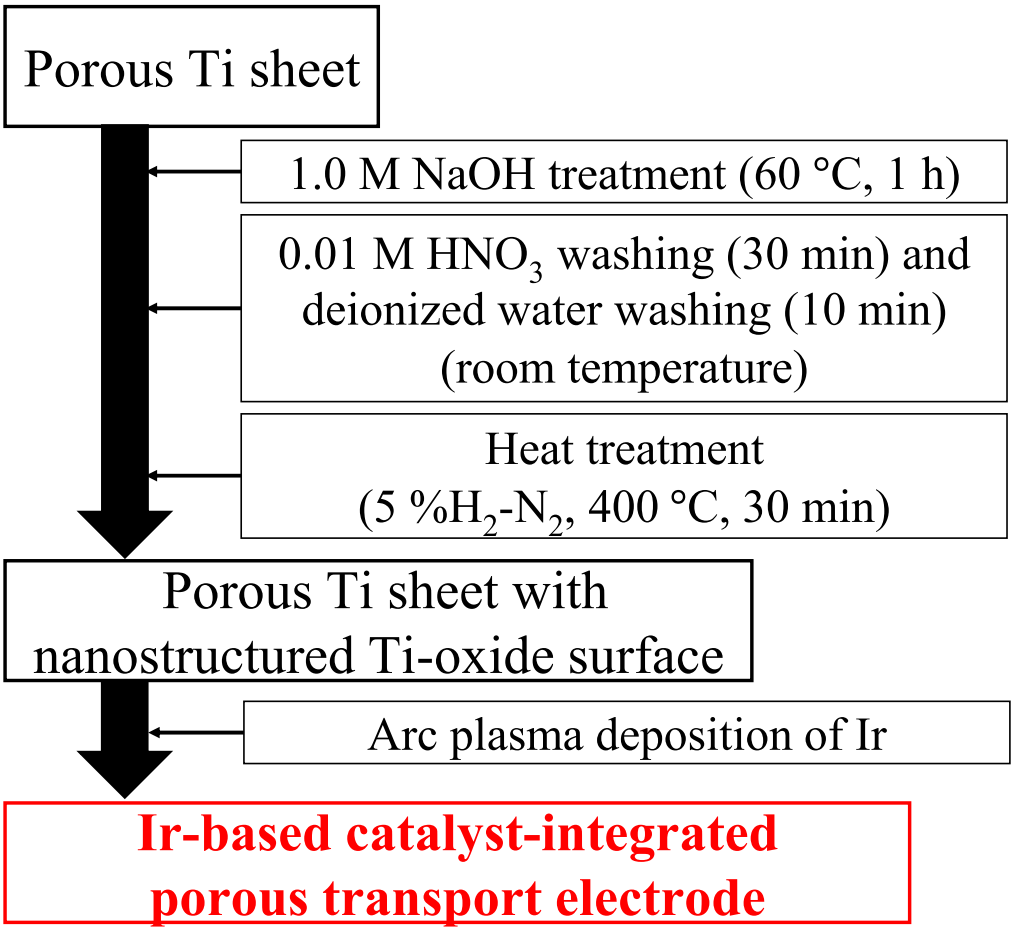

Figure 3. The preparation procedure of the catalyst-integrated PTE.

performed at 400 °C in 5% H_2-N_2 gas (50 ml min^{-1}) for 30 min, with a heating rate of 5 °C min^{-1}. In this etching process, the surface area of PTLs increases from 1.0 m^2 g^{-1} to 1.7 m^2 g^{-1}.[22]

Metallic iridium acting as both a catalyst and a conductive coating on PTLs was deposited onto the NaOH-etched titanium sheets at room temperature via arc plasma deposition (APD-S, Advanced RIKO, Inc., Yokohama, Japan),[23] using a vacuum pressure of 10^{-3} Pa; a discharge voltage of −100 V; a capacitance of 1080 μF; and a discharge frequency of 3 Hz. In the arc plasma deposition (APD), the target material at the surface becomes plasma by discharging an electric charge stored in a capacitor onto the target. The material plasma is deposited on a substrate in front of the target.[23]

Iridium loading was controlled by varying the number of APD pulses.[22] The Ir loading was calculated using a calibration curve obtained by measuring Ir loading per unit area on carbon paper (instead of Ti sheets) by thermogravimetry (Thermo Plus TG8121, Rigaku Co., Tokyo, Japan) in air.[22] First, metallic iridium was deposited onto the carbon papers via APD with various numbers of APD pulses. The Ir loading per unit area and per pulse was then obtained by measuring the mass of iridium after oxidative removal of carbon papers by TG. The measured Ir loading after APD 1000 pulses was 0.043 $mg_{\text{-Ir}}$ cm^{-2}.

Preparation of membrane electrode assemblies (MEAs) with catalyst-integrated PTEs.—Table I summarizes the specification of the water electrolysis cell when using catalyst-integrated PTEs only. MEAs were prepared with an electrode area of 1.0 cm^2 (1 cm by 1 cm) and a Pt loading of 0.5 $mg_{\text{-Pt}}$ cm^{-2} for the PEMWE cathode. Catalyst paste for the PEMWE cathodes was prepared by dispersing the commercial Pt/C catalyst (Pt 46.5 wt%, TEC10E50E, Tanaka Kikinzoku Kogyo Co., Tokyo, Japan), 99.5% ethanol, deionized water, and 5% Nafion solution (Dispersion Solution DE521 CS type, FujiFilm Wako Pure Chemical Corp., Japan) using an ultrasonic homogenizer. The Nafion ratio in the cathode catalyst layer was 28 wt%. This catalyst paste was printed onto the polymer electrolyte membrane (Nafion212, E. I. du Pont de Nemours and Co., Wilmington, USA) using a spray printing system (C-3 J, Nordson Co., Westlake, USA). The catalyst-integrated PTE was applied for the PEMWE anode. The impact of Ir loading on the cell performance up to high current densities was evaluated by varying the Ir loading from 0.043 to 0.086, 0.172, 0.344, and 0.688 mg cm^{-2}. These Ir loadings correspond to 1000, 2000, 4000, 8000, and 16000 pulses of APD.

The MEAs were prepared by hot-pressing this PTE anode, with the electrolyte membrane coated with the Pt/C catalyst layer on the cathode side, at 140 °C at 0.2 MPa for 180 s. Carbon paper (EC-TP1–060T, ElectroChem Inc., Raynham MA, USA) was used as the PTL on the cathode side. No PTL was additionally used for the anode as the catalyst-integrated PTE acts as the PTL. The tightening torque was set to be 4 N m for setting up the PEMWE cells.

Preparation of MEAs with conventional IrO_2 powder catalysts.—Table II summarizes the specification of the water electrolysis cells when using the IrO_2 powder catalyst layer only, the conventional design. The cathode specifications are common for all types of MEAs. The correlation between Ir loading and cell performance was evaluated by varying IrO_2 loading from 0.1 to 0.5 mg cm^{-2}. In order to evaluate the effect of Pt coating on cell performance by varying IrO_2 loading, Pt-coated Ti sheets and Ti sheets without Pt coating were used as PTLs. IrO_2 catalyst paste for the PEMWE anode was prepared by dispersing the IrO_2-based catalyst (IrO_2 (IV) TYPE II, Tokuriki Honten Co. Ltd, Tokyo, Japan), 99.5% ethanol, deionized water, and 5% Nafion solution using an ultrasonic homogenizer. The Nafion ratio to IrO_2 catalyst was 14 wt%. These anode and cathode catalyst pastes were printed onto the electrolyte membrane using the spray printing system. The Pt loading on the cathode was 0.5 mg cm^{-2}, which was the same as when preparing MEAs with catalyst-integrated PTEs, and IrO_2 loading was set to be 0.1 or 0.5 mg cm^{-2}. The MEAs were prepared by hot-pressing the electrolyte membrane, after printing the Pt/C catalyst and the IrO_2 catalyst, at 140 °C at 0.3 MPa for 180 s. Carbon paper (EC-TP1–060T, ElectroChem Inc., Raynham MA, USA) was used as the PTL on the cathode side. Ti fiber sheets with and without Pt coating (Nikko Techno, Ltd, Osaka, Japan) were used as the PTLs on the anode side. The same Ti sheets were used as the substrate, as those used to fabricate catalyst-integrated PTEs. Pt loading on a titanium sheet was 9 mg cm^{-2}. The tightening torque was set to be 4 N m for setting up the PEMWE cells.

Preparation of MEAs with hybrid anodes.—Table III summarizes the specification of water electrolysis cells with the hybrid

Table I. Specifications of water electrolysis cells with the catalyst-integrated PTEs.

	Anode	Cathode
Porous transport layer	Porous Ti sheet after NaOH surface treatment	Carbon paper
Electrode area/cm^2	1	
Electrocatalyst	Ir-based electrocatalyst	46.5 wt% Pt/C
Catalyst loading/mg cm^{-2}	Ir: 0.043 per APD 1000 pulses	Pt: 0.5
Nafion ratio/wt%	(none)	28
Cell temperature/°C	80	
Electrolyte membrane	Nafion® 212 (51 μm in thick)	

Table II. Specifications of water electrolysis cells with the conventional IrO_2 powder catalysts. Total PGM loading in an anode is defined as the sum of metallic iridium and platinum.

	Anode	Cathode
Porous transport layer	Porous Ti sheet with and without Pt coating (9 mg cm^{-2})	Carbon paper
Electrode area/cm^2	1	
Electrocatalyst	IrO_2	46.5 wt% Pt/C
Catalyst loading/mg cm^{-2}	IrO_2: 0.1 or 0.5	Pt: 0.5
Total PGM in anode/mg cm^{-2}	9.086 or 9.429 (IrO_2 (Ir): 0.1 (0.086) or 0.5 (0.429))	
Nafion ratio/wt%	(none)	28
Cell temperature/°C	80	
Electrolyte membrane	Nafion® 212 (51 μm in thick)	

Table III. Specifications of water electrolysis cells with the hybrid anodes. Total PGM loading in an anode is defined as the sum of metallic iridium and platinum.

	Anode	Cathode
Porous transport layer	Porous Ti sheet after the surface treatment	Carbon paper
Electrode area/cm^2	1	
Electrocatalyst	Ir-based electrocatalyst	46.5 wt% Pt/C
Catalyst loading/mg cm^{-2}	Ir catalyst-integrated PTE: 0.344 (8000 APD pulses) IrO_2: 0.1 or 0.3	Pt: 0.5
Total PGM in anode/mg cm^{-2}	0.43 or 0.6 (IrO_2 (Ir): 0.1 (0.086) or 0.3 (0.257))	
Nafion ratio/wt%	(none)	28
Cell temperature/°C	80	
Electrolyte membrane	Nafion® 212 (51 μm in thick)	

anodes. IrO_2 catalyst was used as an intermediate catalyst layer, and the catalyst-integrated PTE was used as an OER-contributing PTL. The cathode preparation condition and the specifications of the Pt/C and IrO_2 catalyst pastes were identical to the other cells. This catalyst paste was printed onto the electrolyte membrane using the spray printing system. The MEAs were prepared by hot-pressing the electrolyte membranes, with the Pt/C and IrO_2 catalysts coated, at 140 °C at 0.3 MPa for 180 s. For the hybrid anodes, 0.1 or 0.3 mg cm^{-2} of IrO_2 was used in the intermediate catalyst layer. Ir loading on the catalyst-integrated PTE was set to be 0.344 mg cm^{-2} (APD: 8000 pulses). Therefore, the total metallic Ir (PGM) loading of the hybrid anode is ca. 0.43 or 0.60 mg cm^{-2}. Carbon paper was used as the PTL on the cathode side. No PTL was additionally used for the anode as the catalyst-integrated PTE acts as the PTL by itself. The tightening torque was set to be 4 N m for setting up the PEMWE cells.

Characterization of MEAs: I-V characteristics and overvoltages.—I-V characteristics of the electrolysis cells were evaluated at 80 °C by supplying high-purity deionized water (Direct-Q UV5, Merck KGaA, Darmstadt, Germany) (18.2 MΩ cm, 20 ml min^{-1}) using a commercial cell holder (Eiwa Corp., Osaka, Japan). Before the electrochemical measurements, deionized water was supplied for 2 d to sufficiently humidify the polymer electrolyte membrane. I-V curves in the high current density range were analyzed by varying voltage from 1.3 V up to around 3.0 V using a bipolar power supply (PBZ20–20A, Kikusui Electronics Corp., Yokohama, Japan) and a data logger (midi LOGGER HV GL2000, Graphtec Corp., Yokohama, Japan). The voltage was held for 5 min at each measurement point, and the average current density value during the last 3 min was taken as the measurement data.

An alternative current (AC) impedance analyzer (1255B, AMETEK Inc., Berwyn, USA) was used to extract ohmic resistance as high-frequency resistance at 20 mA cm^{-2}. Impedance spectra were evaluated at frequencies ranging from 0.1 Hz to 10^6 Hz with an amplitude of 2 mA cm^{-2}. Activation and mass transport overvoltages were then separated along with the typical procedure widely used for PEFC evaluations as follows.[24] A Tafel plot was created with current density on the logarithmic x-axis and the IR-free (ohmic-overvoltage-free) cell voltage on the y-axis. In the low current density region, 6 values were fitted with linear regression. The difference between the theoretical electromotive force (1.17 V at 80 °C, at ambient pressure) and the voltage of the linear regression line was taken as the activation overvoltage at the current density of interest. The deviation of IR-free voltage from the voltage in the linear regression line in the Tafel plot was taken as the mass transport overvoltage.[24] In this study, a reference electrode is not applied so that overvoltage includes both contributions from the anode and the cathode. However, the exchange current density of Pt catalyst for hydrogen evolution reaction (HER) on the cathode side is 1.0×10^{-3} A cm^{-2},[25] which is sufficiently higher compared to 1.6×10^{-7} A cm^{-2} of iridium catalyst to OER on the anode side.[26] In addition, the relatively-high Pt loading on the cathode side was unified to 0.5 mg cm^{-2} for this experiment. Therefore, the difference in each overvoltage in this study arose from the anodes with different fabrication conditions.

Note that the extrapolated ohmic resistance was used in this overvoltage separation, although the actual ohmic resistance could vary due to e.g. the water content fluctuation of the electrolyte membrane, increase in cell temperature,[27] and cell components oxidation under high potential and current density operation around 10 A cm^{-2}.

Characterization of MEAs: Electrochemical surface area (ECSA).—The ECSAs of Ir deposited on the catalyst-integrated PTEs were evaluated, along with the method proposed by National Renewable Energy Laboratory (NREL).[28] As reported in our previous study, the iridium catalyst deposited via APD is metallic iridium.[22] Therefore, the ECSA of metallic iridium can be measured by evaluating the hydrogen desorption peak. The electrical charge of hydrogen adsorbed on metallic Ir per 1 cm^2 is 179 μC. After setting an MEA to the single cell set-up, high-purity deionized water was supplied to the set-up for 2 d to humidify the electrolyte membrane sufficiently. The cell temperature was 80 °C. Remaining water and air in the anode and cathode flow channels were then purged with nitrogen. After the nitrogen purge, hydrogen was supplied to the cathode at 70 ml min^{-1}, while the nitrogen supply to the anode side was stopped. The scanning range of cell potential versus the Pt/C cathode in hydrogen was from 0.025 to 0.55 V for the ECSA evaluation.

Results and Discussion

Catalyst-integrated PTEs: Electrochemical surface area for different iridium loadings.—It is essential to measure the ECSA of newly-developed PTEs in order to compare their respective electrochemical performances. The ECSAs of Ir loaded on catalyst-integrated PTEs was therefore measured to evaluate the correlations between ECSA, activation overvolatage, and mass transport overvoltage. The number after "Ir-" in the sample name indicates the number of APD pulses. Figures 4a–4c show (a) CVs from Ir-1000 to Ir-16000 PTEs, (b) ECSA, and (c) roughness factor for different iridium loadings. The roughness factor is defined as the ECSA multiplied by the iridium loading[12] as widely used in polymer electrolyte fuel cell (PEFC) studies. The clear hydrogen adsorption and desorption peaks around 0.1 V in Fig. 4a confirm that metallic iridium is deposited on the catalyst-integrated PTEs,[28,29] since this peak is not observed for iridium oxide.[28] Our previous study also confirmed the metallic state of iridium deposited by APD via crystallographic analysis.[22]

The ECSA decreases as the Ir loading increases (Fig. 4b). Our previous study showed that the morphology of Ir catalysts deposited by APD varies from individual nanoparticles at low loading to a continuous film at higher loading.[22] Figure 5 shows (a) STEM-EDS images of the Ir catalysts deposited via 8000 pulses and (b-e) the corresponding EDS elemental intensity maps for iridium, titanium, and oxygen. It has been previously noted that TiO_2 nanotubes grow on Ti metals as a result of NaOH etching.[22] These results confirm

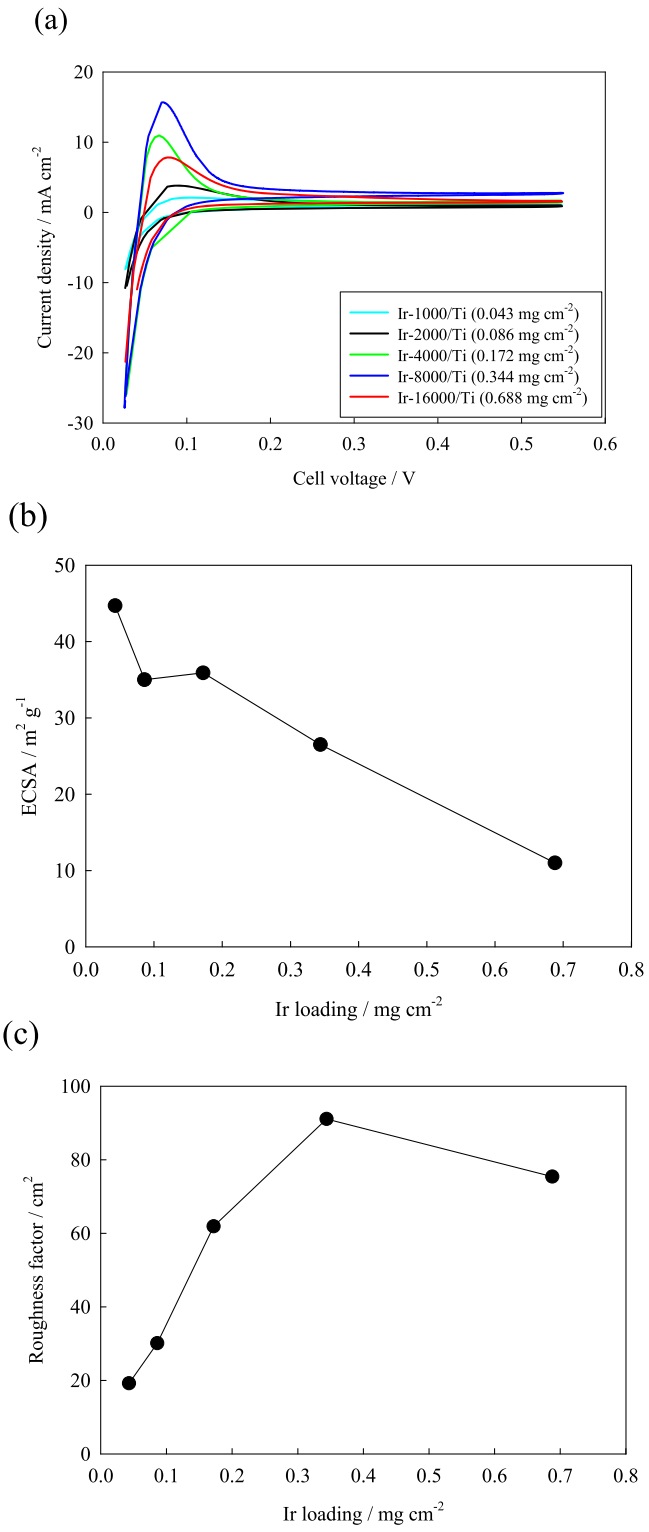

Figure 4. (a) Cyclic voltammograms; (b) correlation between the ECSA and Ir loading; and (c) the correlation between the roughness factor of Ir and Ir loading for the Ir catalyst-integrated PTE with various Ir loadings. The roughness factor is defined as the ECSA multiplied by the iridium loading.

that Ir films (Fig. 5c) cover the Ti-based nanostructure (Fig. 5d), with a film thickness of a few tens of nanometers. Weak oxygen EDS signals in Fig. 5e may be associated with the oxidation of titanium.

Meanwhile, as shown in Fig. 4c, the Ir-8000 PTE sample (Ir loading: 0.344 mg cm^{-2}) has the highest roughness factor, whilst Ir-16000 PTE (Ir loading: 0.688 mg cm^{-2}) has lower roughness factor. This is attributed to the decrease in ECSA with increasing Ir loading, as shown in Fig. 4b. Conventional IrO_2 catalyst powder typically has an ECSA of 15 to 60 m^2 g^{-1}.[28,30–32] As such, as the Ir loading increased, the ECSA of the Ir-deposited catalyst-integrated PTE decreased from 45 to 25 m^2 g^{-1} (i.e. from Ir-1000/Ti to Ir-8000/Ti, Fig. 4b) but is still expected to contribute sufficiently to the OER as a catalyst for electrolysis. The Ir catalyst on the PTL can also act as a conductive coating. Consequently, the design of this PTL is expected to result in reduced PGM loading at the anode, as well as decreasing the activation overvoltage.

However, the trend of decreasing catalyst utilization with increased catalyst loading for the catalyst-integrated PTEs is more clear than that of the conventional catalyst layer. Rozain et al. evaluated the correlation between IrO_2 loading and catalyst utilization in conventional anodes.[33] They defined the surface area of the IrO_2 catalyst layer by the voltametric charge in cyclic voltammograms and observed that the surface area increased linearly up to 2.2 mg cm^{-2}, after which the increase in the surface area began to saturate, suggesting a decrease in catalyst utilization. In the case of the catalyst-integrated PTEs, the catalyst surface area (i.e. the roughness factor) saturates at around 0.344 mg cm^{-2}, as shown in Fig. 4c. In other words, the decrease in catalyst utilization with increasing Ir loading starts in a lower Ir loading region because a change in catalyst geometry occurs at much lower Ir loading on the PTE, as already shown in our previous study.[22]

Catalyst-integrated PTEs: I-V characteristics in the high current density region for different iridium loadings.—The correlation between Ir loading, the overvoltages, and the I-V characteristics of the catalyst-integrated PTEs in the high current density region was also evaluated in MEAs. Figure 6 shows (a) the I-V characteristics and (b) the ohmic, (c) activation, and (d) mass transport overvoltages. The ohmic overvoltage was extrapolated linearly by using high-frequency resistance values measured at 20 mA cm^{-2}, and activation and mass transport overvoltages were separated using this extrapolated ohmic overvoltage. The I-V characteristics in Fig. 6a show that current density at any given cell voltage increases as the Ir loading increases. Meanwhile, a limiting current density is observed in the high current density region.

The ohmic overvoltage exhibited no significant difference between these electrodes (Fig. 6b). In contrast, the activation and mass transport overvoltages do display clear differences. As shown in Fig. 6c, the catalyst-integrated PTE with 2000 APD pulses exhibited the highest activation overvoltage, while the PTEs with 4000, 8000, and 16000 APD pulses exhibited lower activation overvoltages, with 8000 pulses resulting in the lowest activation overvoltage. The roughness factor can be explained by this activation overvoltage trend. In Figs. 4c and 6c, it is observed that the activation overvoltage decreases with increasing roughness factor. The Ir−2000 PTE sample, with the lowest roughness factor, exhibited the highest activation overvoltage. Furthermore, the Ir-4000 and Ir-16000 PTEs, with comparable roughness factors, showed comparable activation overvoltages. The highest roughness factor of the Ir-8000 PTE leads to the lowest activation overvoltage.

Regarding mass transport overvoltage, shown in Fig. 6d, a limiting current density was observed at around 2.0 A cm^{-2} and 7.0 A cm^{-2} for the Ir-2000 and Ir-4000 PTEs, respectively. One possible explanation for this is the rapid formation of oxygen gas which covers the active sites and blocks further electrode reactions.[34] Actually, Taie et al. reported that lower Ir loading on the catalyst layer results in higher mass transport overvoltage. Such phenomena can be understood as being due to the oxygen production rate per specific active area becoming too high for oxygen gas to be removed from the OER sites, causing an accumulation of oxygen gas.[35] Therefore, these electrodes, especially with relatively lower roughness factor (i.e., fewer active sites), tend to exhibit limiting current density behavior at a lower current density.

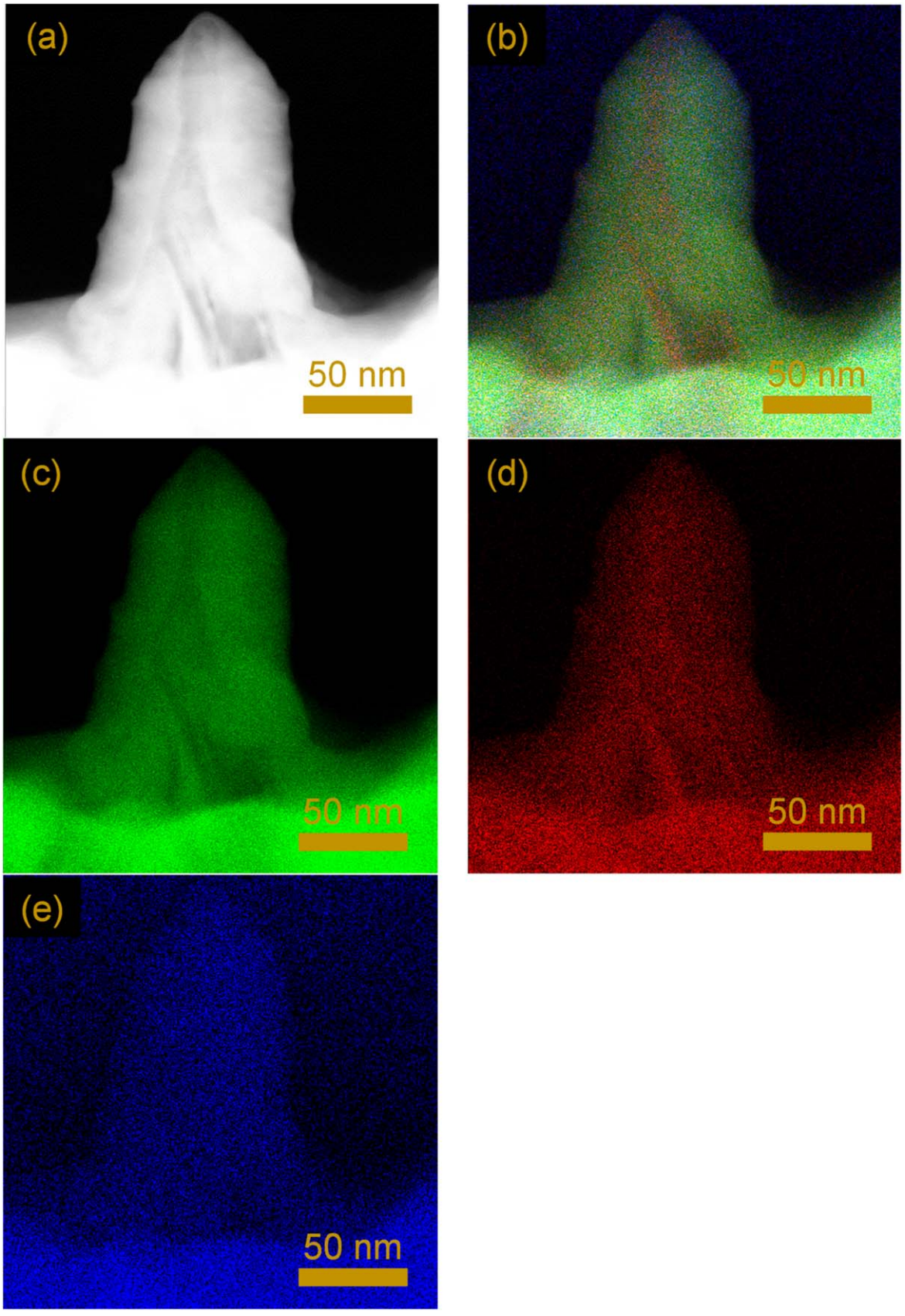

Figure 5. (a) STEM image of the catalyst-integrated PTE prepared via 8000 APD pulses; Corresponding EDS elemental intensity maps for: (b) sum overlapping of iridium, titanium, and oxygen, (c) iridium, (d) titanium, and (e) oxygen.

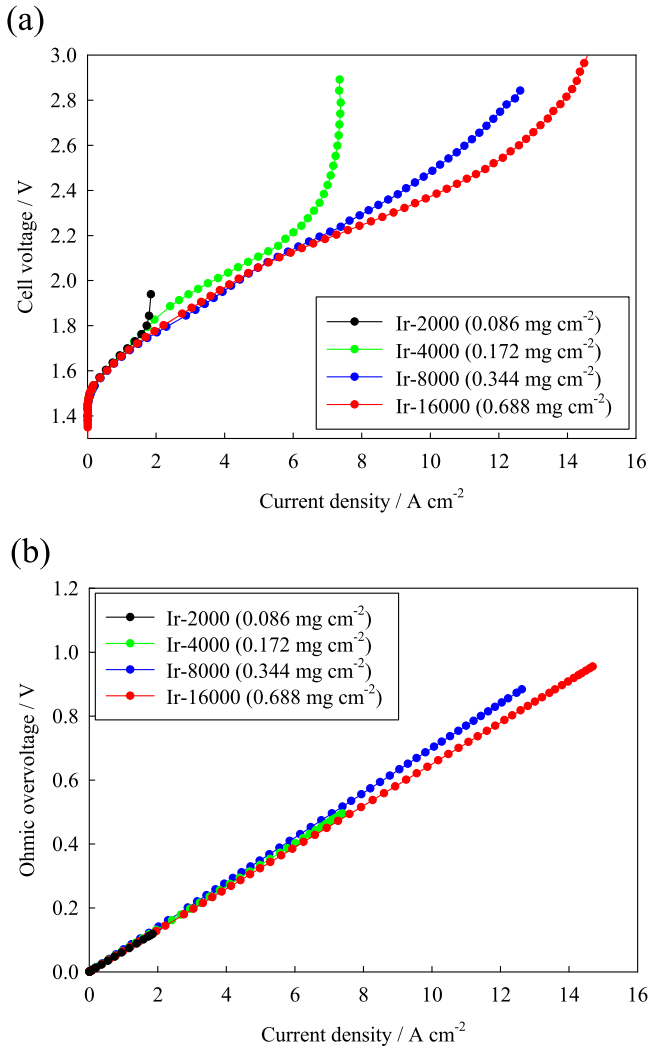

Figure 6. Electrochemical properties of PEMWE cells using catalyst-integrated PTEs prepared with various Ir loading by varying APD pulses: (a) I-V characteristics, (b) ohmic overvoltage, (c) activation overvoltage, and (d) mass transport (concentration) overvoltage. Note that overvoltages were separated by extrapolating ohmic overvoltage measured at 20 mA cm^{-2}.

A decrease in mass transport overvoltage was observed at a current density of around 5 to 10 A cm^{-2} for the Ir-8000 and Ir-16000 PTEs (Fig. 6d). In this study, the ohmic overvoltage determined at 20 mA cm^{-2} was extrapolated to higher current density. Therefore, a decrease in ohmic overvoltage due to an increase in proton conductivity of the electrolyte membrane and a decrease in activation overvoltage due to an increase in catalytic activity at higher cell temperatures are expected in such high current density operation.[27] An increase in cell temperature in such a high current density region leads to an apparent decrease in mass transport overvoltage.

Conventional IrO_2 catalyst anodes.—While a catalyst-integrated PTE was prepared as an alternative to conventional Pt-coated PTLs, it is essential to analyze the impact of Pt coating on cell performance to clarify the effectiveness of catalyst-integrated PTEs and highlight any issues that may arise. The performances of MEAs using a titanium PTL with and without a Pt coating are herein compared to evaluate the effect of Pt coating on cell performance especially in the high current density operation. Figure 7 shows (a) the I-V characteristics and (b-d) overvoltages with different IrO_2 loadings from 0.1 to 0.5 mg cm^{-2}. The cell using the conventional IrO_2 catalyst without Pt coating in the PTL exhibited a significantly lower current density at any given cell voltage and instable cell voltage at high current densities (Fig. 7a). The reasons for such poor performance could be explained with respect to each overvoltage.

First, the effect of IrO_2 loading on ohmic overvoltage is considered (Fig. 7b). With the Pt coating on the PTL, the ohmic overvoltages of the MEAs with 0.1 and 0.5 mg cm^{-2} IrO_2 loading are comparable. In contrast, without the Pt coating on the PTL, the ohmic overvoltage increased for both IrO_2 loadings. This may be because of a decrease in the electrical conductivity of the PTL itself without Pt coating. In addition, the increased interfacial resistance between the catalyst layer and the PTL could also cause this increase in ohmic overvoltage. The increase in ohmic overvoltage for the cell with an IrO_2 loading of 0.1 mg cm^{-2} was more pronounced than for 0.5 mg cm^{-2}. A reduction in the in-plane conductivity in the case of low IrO_2 loading could also contribute to this increase in ohmic overvoltage. At high current densities and without Pt coating, oxidation of titanium may be promoted, increasing ohmic resistance and leading to instable cell voltage (Fig. 7). As mentioned before, many studies have noted a decrease in the in-plane electrical conductivity of catalyst layers at low iridium loading.[10,13,33,36] In particular, Lopata et al. evaluated the effect of the PTL microstructure on cell performance using IrO_2 anode catalysts at low and high Ir loadings of 0.085 mg cm^{-2} and 0.595 mg cm^{-2} to understand the effect of the interface between the catalyst layer and the porous transport layer (CL/PTL).[14] According to their study, the dependence of cell performance on PTL microstructure was more pronounced at a low Ir loading, and the ohmic overvoltage for low iridium loading was higher than that for high iridium loading. Therefore, the low in-plane conductivity of the low-iridium-loading catalyst layer could significantly affect the CL/PTL interfacial contact and, thus cell performance.[14] In this study, the lower IrO_2 loading also causes higher ohmic overvoltage, indicating lower in-plane conductivity.

The activation overvoltage was also analyzed (Fig. 7c). Cells with 0.1 mg cm^{-2} of relatively low IrO_2 loading and a PTL without Pt coating exhibited higher activation overvoltage than when using the PTL with Pt coating. As discussed earlier, the lower IrO_2 loading results in lower in-plane conductivity in the catalyst layer. When both the in-plane conductivity of the catalyst layer and the conductivity of the PTL are low, the contact resistance at the CL/PTL interface is more pronounced, resulting in a significant decrease in catalyst utilization and a considerable increase in activation overvoltage.[11,12] The catalyst layer with higher IrO_2 loading of 0.5 mg cm^{-2} may exhibit a higher in-plane conductivity. Such high in-plane conductivity could result in high catalyst utilization affecting activation overvoltage, even when using a titanium PTL without the Pt coating.

Finally, the mass transport overvoltage is discussed, especially the effect of Pt coating on the limiting current density (Fig. 7d). For the cell with 0.1 mg cm^{-2} of conventional IrO_2 catalyst, the limiting current densities with and without Pt coating on the PTL were 9.1 and 3.5 A cm^{-2}, respectively. Lower catalyst utilization, caused by higher interfacial resistance between the catalyst layer and the Pt-coating-free PTL, resulted in a lower limiting current density. Even at the IrO_2 loading of 0.5 mg cm^{-2}, the limiting current density with a Pt-coating-free PTL was about 8.0 A cm^{-2}, but no apparent limiting current density was observed with the Pt-coated PTL, showing that the limiting current density can be significantly increased by using the Pt coating. The activation overvoltage separated from the ohmic overvoltage in low current density region remained comparable with and without the Pt coating, indicating a comparable catalyst utilization at lower current density. However, oxidation of the Ti sheets may occur during the electrolysis test up to high voltage at higher current density. In fact, the ohmic resistance increased significantly from 0.08 Ω cm^2 to 0.175 Ω cm^2 after I-V measurements at high current density, indicating oxidization or dissolution of the titanium PTL. Such an increase in ohmic resistance could result in a decrease in catalyst utilization, leading to a lower limiting current density with the Pt-coating-free PTL.

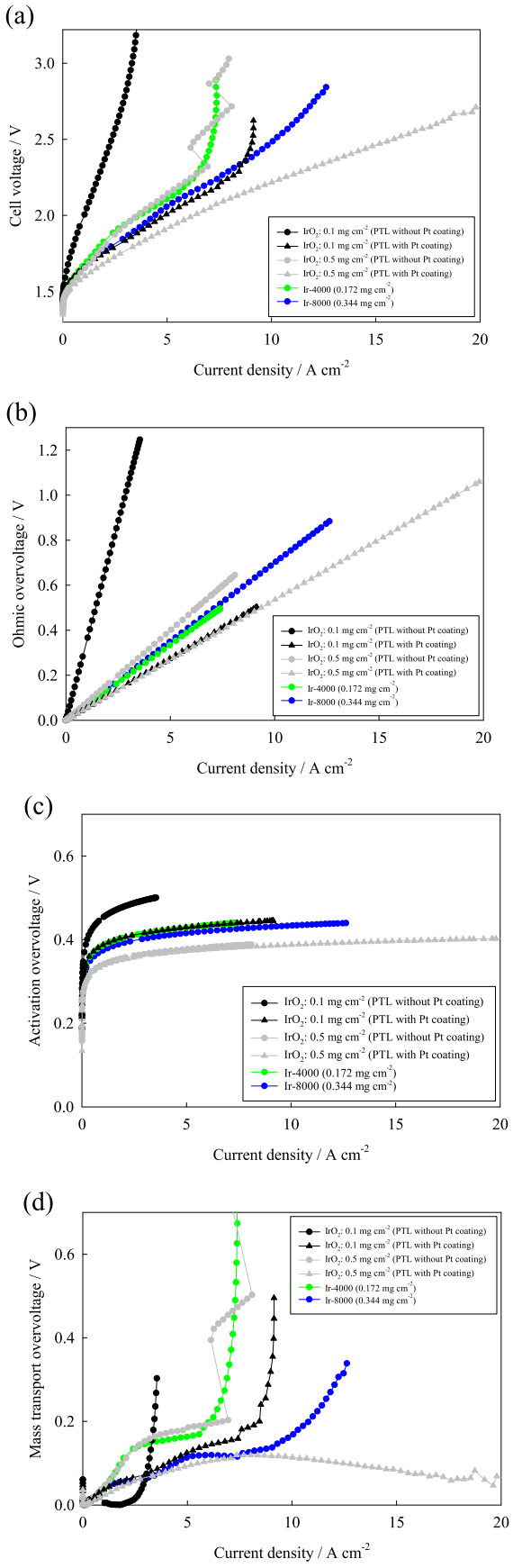

Figure 7. Electrochemical properties of PEMWE cells using the Ir catalyst-integrated PTEs with different Ir loadings and the conventional IrO_2 anodes with and without Pt coating on titanium PTLs: (a) I-V characteristics, (b) ohmic overvoltage, (c) activation overvoltage, and (d) mass transport (concentration) overvoltage. Note that overvoltages were separated by extrapolating ohmic overvoltage measured at 20 mA cm^{-2}.

Comparison between the catalyst-integrated PTEs and the conventional IrO_2 catalyst anodes.—In this section, the catalyst-integrated PTE is now compared with the conventional IrO_2 powder-based anode. The I-V performance of the cell with the catalyst-integrated PTE (Ir-4000 and Ir-8000) in Fig. 7a exhibits higher performance than that using the conventional IrO_2 catalyst (IrO_2 loading: 0.1 mg cm^{-2}) with the Pt-coating-free PTL. However, the performance with the catalyst-integrated PTE is still not as high as that of the cells using the conventional IrO_2 with a loading of 0.5 mg cm^{-2} with the Pt-coated PTL, as shown in Fig. 7a. The reasons of such cell performance difference are considered by analyzing the overvoltages.

As shown in Fig. 7b, the catalyst-integrated PTE shows higher ohmic overvoltage than the conventional IrO_2 anode with the Pt-coated PTL. With such catalyst-integrated PTEs, the proton transport resistance between the polymer electrolyte membrane and the electrode is higher due to a lower contact area between the electrolyte membrane and the electrode.[37] In contrast, the ohmic resistance of the catalyst-integrated PTE is lower than that using the conventional IrO_2 catalyst with the Pt-coating-free PTL. This may be because the CL/PTL contact resistance of the catalyst-integrated PTE is expected to be minimized by depositing Ir catalyst directly on the PTL, improving electrical contact.

The activation overvoltages of the cell using the Pt-coated PTL with a conventional IrO_2 catalyst layer, and the cell using the catalyst-integrated PTE are herein compared. As shown in Fig. 7c, the catalyst-integrated PTE with 0.172 mg cm^{-2} (Ir-4000) and 0.344 mg cm^{-2} (Ir-8000) Ir loading exhibited comparable activation overvoltages, which are similar or slightly lower compared to the conventional electrode using 0.1 mg cm^{-2} of IrO_2 catalysts with the Pt-coated PTL. The Pt loading for the PTL coating in this study was 9.0 mg cm^{-2}, and its value is higher than a typical Pt loading of 1 to 5 mg cm^{-2}. This relatively-high Pt loading aims to eliminate the cell performance degradation from incomplete Pt coating on PTL. The total PGM loading of the conventional anode was therefore ca. 9.1 mg cm^{-2} (IrO_2 catalyst: 0.1 mg cm^{-2}, Pt coating: 9 mg cm^{-2}), while a typical Pt loading is ca. 1 to 5 mg cm^{-2}. In contrast, the total PGM loading of the catalyst-integrated PTE was 0.172 or 0.344 mg cm^{-2}, confirming that the OER-active PTL can significantly reduce overall PGM loading. The reduction in activation overvoltage by increasing the Ir loading for the catalyst-integrated PTE was relatively small, and thus the overvoltage was still higher than the cell using 0.5 mg cm^{-2} of the conventional IrO_2 catalyst and the Pt-coated PTL.

As shown in Fig. 7d, the limiting current density using the catalyst-integrated PTEs was often higher than that using the conventional IrO_2 catalyst layers. The higher limiting current density indicates that this unique highly porous structure of the catalyst-integrated PTE can maintain high catalyst utilization and enables high current density operation. However, the issue of the catalyst-integrated PTE still remained is that increasing the Ir loading lowers the ECSA, resulting in a lower limiting current density and a higher mass transport overvoltage than the cell with the conventional IrO_2 catalysts and the Pt-coated PTL.

Hybrid anodes with both the IrO_2 catalysts and the catalyst-integrated PTEs.—The catalyst-integrated PTE can be operated at a higher current density with a low Ir loading and without Pt coating on the PTL. However, higher activation overvoltage is still an issue at a higher Ir loading, where the ECSA of the catalyst-integrated PTE decreases. This is because APD deposits the Ir catalyst on PTL as a thin film, leading to a lower ECSA for higher Ir loadings. In addition, the higher ohmic overvoltage is also an issue due to a higher proton transport resistance between the electrolyte membrane and the catalyst-integrated PTE. A novel hybrid anode could solve these issues, where an intermediate catalyst layer is introduced between the electrolyte membrane and the catalyst-integrated PTE,

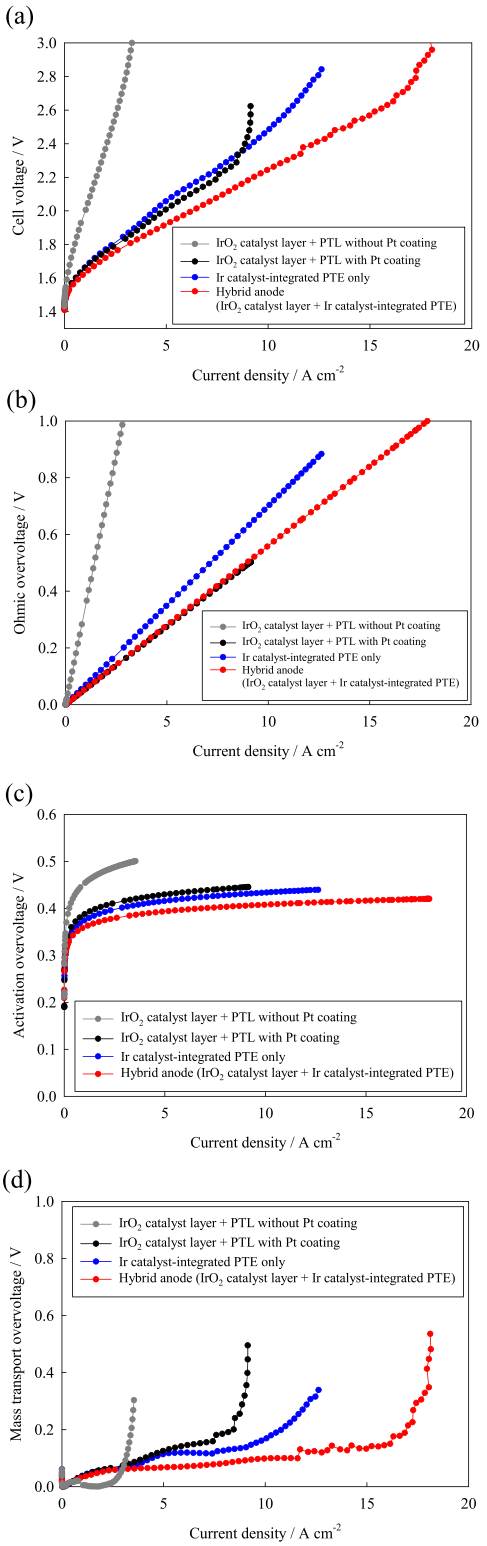

Figure 8. Electrochemical properties of PEMWE cells using the hybrid anode, the Ir catalyst-integrated PTE only, and the conventional IrO_2 anodes with and without Pt coating on titanium PTLs. IrO_2 loading for the catalyst layer of the hybrid anode and the conventional anode was set to be 0.1 mg cm^{-2}. Ir loading on the Ir catalyst integrated PTE was set to be 0.344 mg cm^{-2}: (a) I-V characteristics, (b) ohmic overvoltage, (c) activation overvoltage, and (d) mass transport (concentration) overvoltage. Note that overvoltages were separated by extrapolating ohmic overvoltage measured at 20 mA cm^{-2}.

as schematically described in Fig. 1. The possible advantages of this novel anode design are as follows.

First, the hybrid structure could decrease the activation overvoltage because both the intermediate catalyst layer and the catalyst-integrated PTE are active towards the OER. The decrease in activation overvoltage by increasing the Ir loading is limited to the catalyst-integrated PTE structure only. Instead of increasing iridium loading in the catalyst-integrated PTE, introducing the intermediate catalyst layer effectively increases the roughness factor per unit PGM loading in the cell, reducing the activation overvoltage.

Secondly, the intermediate catalyst layer is expected to decrease the ohmic overvoltage due to better electrical contact between the electrolyte membrane and the catalyst-integrated PTE. The intermediate catalyst layer is an excellent mixed protonic and electronic conductor consisting of Nafion ionomer and IrO_2, improving the protonic and electronic transport at the interface.

Thirdly, this novel structure is expected to reduce the total PGM loading. As described above, cell performance degradation is inevitable without Pt loading on PTLs. In this scheme, this hybrid electrode can be made virtually Pt-free without increasing the total iridium loading, for hybrid and conventional anodes with the same iridium loading and electrolysis performance. This hybrid anode could be therefore an effective concept for reducing total PGM usage in PEMWEs.

Table III shows the specifications in using this hybrid anode. The hybrid anode consists of the catalyst-integrated PTE with 0.344 mg cm^{-2} Ir loading (Ir-8000) and the intermediate catalyst layer with 0.1 mg cm^{-2} IrO_2 loading.

First, it is essential to verify the OER contribution of Ir as a catalyst on the catalyst-integrated PTE in this hybrid anode concept. Cells using the PTL with and without Pt coating, the catalyst-integrated PTE (Ir-8000) only, and the hybrid anode consisting of the IrO_2 catalyst layer and the catalyst-integrated PTE are all compared. The IrO_2 loading for the catalyst layer of the hybrid anode and the conventional anode (IrO_2 catalyst layer + PTL with Pt coating) was set to be 0.1 mg cm^{-2}. Figure 8 shows their (a) I-V characteristics and (b-d) overvoltages. The hybrid anode exhibited the highest electrolysis performance as shown in Fig. 8a. Since the hybrid anode replaced the Pt-coated PTL with the Ir catalyst-integrated PTE, this performance improvement is assumed to originate from the use of the Ir catalyst-integrated PTE. The contribution of the hybrid anode to each overvoltage is described as follows.

Figure 8b shows the ohmic overvoltage of each electrode. The use of the hybrid anode reduces ohmic overvoltage to a comparable level with the conventional anode. The comparison between the hybrid anode and the anode using PTL without Pt coating indicates that Ir coating on the catalyst-integrated PTL reduces the electrical resistance at the CL/PTL interface. In addition, the mixed (ionic and electronic) conducting intermediate catalyst layer of the hybrid anode may suppress the proton transfer resistance at the PEM/PTE interface, which has to be taken into account when comparing the hybrid anode and the Ir catalyst-integrated PTL only.

Figures 8c and 8d show the activation and mass transport overvoltage of each electrode, respectively. Notably, the activation and mass transport overvoltages of the hybrid anode were lower than that of the conventional anode with the Pt-coated PTL and the catalyst-integrated PTE only. IrO_2 loadings of the catalyst layer of the conventional anode and the hybrid anode are the same. Therefore, the reduction of the activation overvoltage but with the same IrO_2 loading clearly indicate that Ir on the catalyst-integrated PTL acts as an OER catalyst, besides a conductive coating. This hybrid structure effectively reduces the activation overvoltage. Hybrid anode also reduces the mass transport overvoltage, as shown in Fig. 8d. This could be because of an increase in the roughness factor on the hybrid anode, such that more OER active sites are available for oxygen gas to be produced and removed.

PGM reduction of PEMWEs.—The hybrid anode structure effectively reduced overvoltages without additional Pt coating on PTLs. However, iridium is much more expensive than platinum. Therefore, if Ir loading and electrolysis performance are the same in both conventional and hybrid anodes, the hybrid anode is advantageous because Pt coating is no longer needed.

The Ir loading and electrolysis performance of the hybrid and conventional anodes is compared in Table IV. Two types of the hybrid anodes with low and high IrO_2 loadings (0.1 and 0.3 mg cm^{-2}) for the intermediate catalyst layer were prepared. The Ir loading on the catalyst-integrated PTEs in the hybrid anodes was unified to 0.344 mg cm^{-2} (Ir-8000). The conventional anode consisting of 0.5 mg cm^{-2} of IrO_2 catalyst and Pt-coated PTL was also used for this comparison. Total PGM loadings of the hybrid anodes (low and high IrO_2 loading) and the conventional anode are 0.43, 0.6, and 9.429 mg cm^{-2}, respectively.

Figure 9 shows the (a) I-V characteristics and (b-d) overvoltages. Even though both hybrid anodes (0.1 and 0.3 mg cm^{-2} IrO_2 loading in the intermediate catalyst layer) do not have Pt-coatings and use significantly less total PGM loading, both hybrid anodes exhibited I-V characteristics equivalent to those of the anode using the Pt-coated PTL (Pt loading: 9 mg cm^{-2}) with an IrO_2 loading of 0.5 mg cm^{-2}, as shown in Fig. 9a. The ohmic overvoltage is also comparable in all these electrodes, as shown in Fig. 9b. However, the hybrid anode with 0.1 mg cm^{-2} of IrO_2 catalyst (total Ir loading: 0.43 mg cm^{-2}) exhibited higher activation and mass transport overvoltages compared to the conventional anode (total Ir loading: 0.429 mg cm^{-2}) as shown in Figs. 9c and 9b. The high activation overvoltage could be related to the roughness factor (ECSA × Ir loading) of Ir on the anode. The total Ir loading of 0.43 mg cm^{-2} on this anode is almost the same as that of 0.429 mg cm^{-2} in the conventional anode. However, the ECSA of Ir on the PTE in the hybrid anode is relatively low, leading to low roughness factor and thus high activation and mass transport overvoltage.

The hybrid anode consisting of 0.3 mg cm^{-2} of IrO_2 intermediate catalyst layer exhibited comparable activation and mass transport overvoltages to the conventional anode (IrO_2 0.5 mg cm^{-2}, Pt-coated PTL), probably due to higher roughness factor by increasing IrO_2 loading to 0.3 mg cm^{-2}. The hybrid anode with 0.1 mg cm^{-2} IrO_2 catalyst exhibited a limiting current density at around 18 A cm^{-2}, but the hybrid anode with a higher loading of 0.3 mg cm^{-2} IrO_2 catalyst (total Ir loading: 0.6 mg cm^{-2}) exhibited no increase in mass transport overvoltage even at the very high current density of 20 A cm^{-2}. While Lewinski et al. have already demonstrated such high current density electrolysis at around 20 A cm^{-2} by applying the NSTF electrode,[38] the unique feature of this hybrid anode is such high current density operation with virtually no Pt coating on the PTL, leading to a lower PGM loading per hydrogen production capacity (g_{PGM}/kW). Further reduction of

Table IV. PGM loadings of the hybrid and conventional anodes used for comparison in Fig. 9. Two types of hybrid anodes with low and high IrO_2 loading for catalyst layers were prepared. Total PGM loading in the anodes is defined as the sum of metallic iridium and platinum.

	Hybrid anode with low IrO_2 loading for CL	Hybrid anode with high IrO_2 loading for CL	Conventional anode
Ir loading on CL (mg cm^{-2})	0.086 (IrO_2: 0.1)	0.257 (IrO_2: 0.3)	0.429 (IrO_2: 0.5)
Pt loading on PTL (mg cm^{-2})	(none)	(none)	9
Ir loading on PTL (mg cm^{-2})	0.344	0.344	(none)
Total Ir loading (mg cm^{-2})	0.43	0.6	0.429
Total PGM loading (mg cm^{-2})	0.43	0.6	9.429

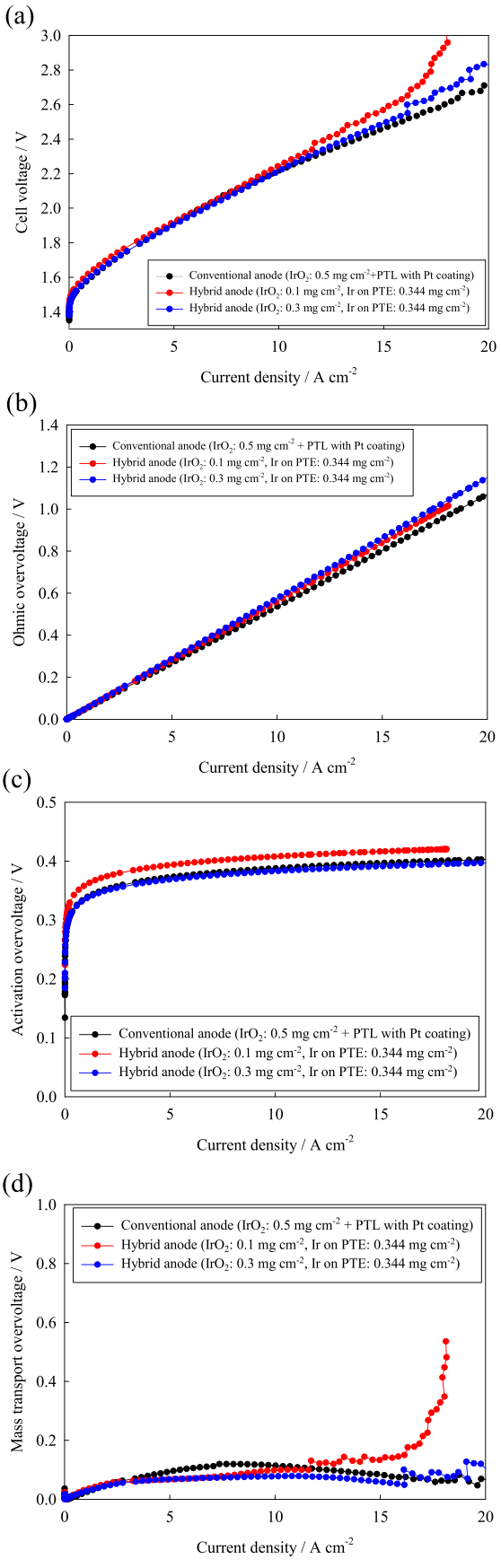

Figure 9. Electrochemical properties of PEMWE cells using the hybrid anodes with the catalyst-integrated PTE, and the conventional anode with 0.5 mg cm^{-2} of IrO_2 loading and the Pt-coated PTL. The Pt loading on the Pt-coated PTL was 9 mg cm^{-2} in this study. IrO_2 loadings for the catalyst layer of the hybrid anode were 0.1 or 0.3 mg cm^{-2}. Ir loading on the Ir catalyst-integrated PTE was 0.344 mg cm^{-2}: (a) I-V characteristics, (b) ohmic overvoltage, (c) activation overvoltage, and (d) mass transport (concentration) overvoltage. Note that overvoltages were separated by extrapolating ohmic overvoltage measured at 20 mA cm^{-2}.

the total Ir loading of the hybrid anode will be possible e.g. by improving the ECSA of Ir on the PTL.

Consequently, the novel Pt-coating-free hybrid anode has demonstrated comparable electrolysis performance to the conventional cell using the Pt-coated PTL, without increasing Ir loading. This hybrid anode does not require the 1 to 5 mg cm^{-2} Pt coating currently used in conventional PTLs. The use of these hybrid anodes reduces the PGM loading, and thus also reduces the CAPEX for PEM water electrolysis. Since the total iridium loading of the hybrid anode (0.43 to 0.6 mg cm^{-2}) is still high, optimizing iridium loading and improving catalytic activity of the hybrid anodes are still needed in future studies to meet an ideal PGM loading target of 0.2 mg cm^{-2}.[2]

Conclusions

In this study, we have developed a novel hybrid anode consisting of an intermediate catalyst layer and a catalyst-integrated PTE. The catalyst-integrated PTE itself was suffered from high activation overvoltage due to reduced ECSA at high Ir loadings. The hybrid anode exhibited lower activation overvoltage and higher limiting current density than a conventional anode with the same Ir loading for the catalyst layer. This lower overvoltage demonstrated that deposited Ir on PTLs acts as both a catalyst and a thin conductive coating, eliminating Pt coating on PTLs. This concept enables electrolysis at a high current density up to 20 A cm^{-2} at a relatively-low iridium usage of ca. 0.4 to 0.6 mg cm^{-2}. This hybrid anode design offers new possibilities for ideal low-PGM and high current density operation for CAPEX reduction of PEMWEs. Further improvement to increase ECSA of Ir on catalyst-integrated PTE may enable even lower PGM loading and higher current density operation of PEM water electrolysis.

Acknowledgments

Financial support from the Center of Innovation (COI) Program by the Japan Science and Technology Agency (JST) is gratefully acknowledged (Grant Number: JPMJCE1318). Partial financial support by the Fukuoka Strategy Conference for Hydrogen Energy and the Kyushu University Q-PIT Support Program for Young Researchers and Doctoral Students is also acknowledged.

ORCID

Masahiro Yasutake https://orcid.org/0009-0006-3032-987X
Akari Hayashi https://orcid.org/0000-0003-1753-2241
Kazunari Sasaki https://orcid.org/0000-0002-3174-9087

References

1. Hydrogen Council, (2017), Hydrogen scaling up: a sustainable pathway for the global energy transition. https://hydrogencouncil.com/wp-content/uploads/2017/11/Hydrogen-Scaling-up_Hydrogen-Council_2017.compressed.pdf (accessed 2023. 1. 4).
2. The International Renewable Energy Agency, (2020), https://irena.org/-/media/Files/IRENA/Agency/Publication/2020/Dec/IRENA_Green_hydrogen_cost_2020.pdf (accessed 2023. 1. 4).
3. The International Renewable Energy Agency, (2020), https://irena.org/-/media/Files/IRENA/Agency/Publication/2020/Jun/IRENA_Costs_2019_EN.pdf?la=en&hash=BFAAB4DD2A14EDA7329946F9C3BDA9CD806C1A8A (accessed 2023. 1. 4).
4. J. E. Park et al., *Nano Energy*, **58**, 158 (2019).
5. H. N. Nong, L. Gan, E. Willinger, D. Teschner, and P. Strasser, *Chem. Sci.*, **5**, 2955 (2014).
6. H. N. Nong, H. S. Oh, T. Reier, E. Willinger, M. G. Willinger, V. Petkov, D. Teschner, and P. Strasser, *Angew. Chemie - Int. Ed.*, **54**, 2975 (2015).
7. S. M. Alia, S. Shulda, C. Ngo, S. Pylypenko, and B. S. Pivovar, *ACS Catal.*, **8**, 2111 (2018).
8. C. Liu, M. Carmo, G. Bender, A. Everwand, T. Lickert, J. L. Young, T. Smolinka, D. Stolten, and W. Lehnert, *Electrochem. Comm.*, **97**, 96 (2018).
9. C. Liu et al., *Adv. Energy Mater.*, **11**, 2002926 (2021).
10. C. Rozain, E. Mayousse, N. Guillet, and P. Millet, *Appl. Catal. B Environ.*, **182**, 123 (2016).
11. T. Schuler, R. De Bruycker, T. J. Schmidt, and F. N. Büchi, *J. Electrochem. Soc.*, **166**, F270 (2019).
12. T. Schuler, T. J. Schmidt, and F. N. Büchi, *J. Electrochem. Soc.*, **166**, F555 (2019).
13. M. Bernt, A. Siebel, and H. A. Gasteiger, *J. Electrochem. Soc.*, **165**, F305 (2018).
14. J. Lopata, Z. Kang, J. Young, G. Bender, J. W. Weidner, and S. Shimpalee, *J. Electrochem. Soc.*, **167**, 064507 (2020).
15. M. Bernt, C. Schramm, J. Schröter, C. Gebauer, J. Byrknes, C. Eickes, and H. A. Gasteiger, *J. Electrochem. Soc.*, **168**, 084513 (2021).
16. A. Villagra and P. Millet, *Int. J. Hydrogen Energy*, **44**, 9708 (2019).
17. D. Kawachino, Z. Noda, J. Matsuda, A. Hayashi, and K. Sasaki, *ECS Trans.*, **80**, 781 (2017).
18. M. Yasutake, H. Anai, D. Kawachino, Z. Noda, J. Matsuda, K. Ito, A. Hayashi, and K. Sasaki, *ECS Trans.*, **86**, 673 (2018).
19. D. Kawachino, M. Yasutake, H. Odoi, Z. Noda, J. Matsuda, A. Hayashi, and K. Sasaki, *ECS Trans.*, **86**, 541 (2018).
20. M. Yasutake, D. Kawachino, Z. Noda, J. Matsuda, K. Ito, A. Hayashi, and K. Sasaki, *ECS Trans.*, **92**, 833 (2019).
21. D. Kawachino, M. Yasutake, Z. Noda, J. Matsuda, S. M. Lyth, A. Hayashi, and K. Sasaki, *J. Electrochem. Soc.*, **167**, 104513 (2020).
22. M. Yasutake, D. Kawachino, Z. Noda, J. Matsuda, S. M. Lyth, K. Ito, A. Hayashi, and K. Sasaki, *J. Electrochem. Soc.*, **167**, 124523 (2020).
23. Y. Agawa, M. Kunimatsu, T. Ito, Y. Kuwahara, and H. Yamashita, *ECS Electrochem. Lett.*, **4**, F57 (2015).
24. M. Okumura, Z. Noda, J. Matsuda, Y. Tachikawa, M. Nishihara, S. M. Lyth, A. Hayashi, and K. Sasaki, *J. Electrochem. Soc.*, **164**, F928 (2017).
25. P. Choi, D. G. Bessarabov, and R. Datta, *Solid State Ionics*, **175**, 535 (2004).
26. M. H. Miles, E. A. Klaus, B. P. Gunn, J. R. Locker, W. E. Serafin, and S. Srinivasan, *Electrochim. Acta*, **23**, 521 (1978).
27. M. Yasutake, Z. Noda, Y. Tachikawa, S. M. Lyth, J. Matsuda, M. Nishihara, K. Ito, A. Hayashi, and K. Sasaki, *ECS Trans.*, **109**, 437 (2022).
28. S. M. Alia, K. E. Hurst, S. S. Kocha, and B. S. Pivovar, *J. Electrochem. Soc.*, **163**, F3051 (2016).
29. S. Motoo and N. Furuya, *J. Electroanal. Chem.*, **167**, 309 (1984).
30. F. Bizzotto, J. Quinson, A. Zana, J. J. K. Kirkensgaard, A. Dworzak, M. Oezaslan, and M. Arenz, *Catal. Sci. Technol.*, **9**, 6345 (2019).
31. S. M. Alia, B. Rasimick, C. Ngo, K. C. Neyerlin, S. S. Kocha, S. Pylypenko, H. Xu, and B. S. Pivovar, *J. Electrochem. Soc.*, **163**, F3105 (2016).
32. S. M. Alia and G. C. Anderson, *J. Electrochem. Soc.*, **166**, F282 (2019).
33. C. Rozain, E. Mayousse, N. Guillet, and P. Millet, *Appl. Catal. B Environ.*, **182**, 153 (2016).
34. J. K. Lee, C. H. Lee, K. F. Fahy, B. Zhao, J. M. LaManna, E. Baltic, D. L. Jacobson, D. S. Hussey, and A. Bazylak, *Cell Reports Phys. Sci.*, **1**, 100147 (2020).
35. Z. Taie, X. Peng, D. Kulkarni, I. V. Zenyuk, A. Z. Weber, C. Hagen, and N. Danilovic, *ACS Appl. Mater. Interfaces*, **12**, 52701 (2020).
36. X. Peng, P. Satjaritanun, Z. Taie, L. Wiles, A. Keane, C. Capuano, I. V. Zenyuk, and N. Danilovic, *Adv. Sci.*, **8**, 1 (2021).
37. C. Capuano et al., *ECS Meet. Abstr.*, **MA2020-02**, 2447 (2020).
38. K. A. Lewinski, D. van der Vliet, and S. M. Luopa, *ECS Trans.*, **69**, 893 (2015).